

# Automated System for Selective Etching of the $\text{Al}_x\text{Ga}_{1-x}\text{As}/\text{GaAs}$ System and Some Applications

M. A. Sagiore, S. Pádua, and F. M. Matinaga

*Departamento de Física, Instituto de Ciências Exatas, Universidade Federal de Minas Gerais, 30123-970, Caixa Postal 702, Belo Horizonte, MG, Brazil*

L. H. F. Andrade

*Laboratório de Física Aplicada, CDTN/CNEN, 30123-970, Belo Horizonte, MG, Brazil*

Recebido em 23/10/2003. Versão revisada recebida em 20/03/2005. Aceito para publicação em 25/03/2005

A simple and fast method to remove semiconductor substrates from epitaxially grown thin films can be very useful for studies of their optical properties. After substrate removal it is possible to make optical transmission studies, investigate ultra-fast time-resolved spectroscopy in semiconductors, and also measure the propagation time of photons in microcavities. In this work, we developed a simple and fast method to remove GaAs substrates in  $\text{Al}_x\text{Ga}_{1-x}\text{As}/\text{GaAs}$  systems using an electro-optical controlled etching jet. The prepared surface with this method present good optical quality and it is well suited for optical studies. Some examples of works that can be done after sample preparation are presented to reinforce the etching precision of this technique. The same system can be used for etching other substrates with its corresponding etching solution and electro-optical relation.

## I. INTRODUCTION

There is a need for a fast and simple method for selective chemical etching able to prepare optical windows in GaAs semiconductor substrates over which are grown thin films of  $\text{Al}_x\text{Ga}_{1-x}\text{As}$  or related devices structures. This is necessary for making optical transmission studies of  $\text{Al}_x\text{Ga}_{1-x}\text{As}$ <sup>1,2</sup>. The etching solution must remove selectively the GaAs substrate without removing the  $\text{Al}_x\text{Ga}_{1-x}\text{As}$  film.

This make us to define a coefficient known as the selectivity of the solution  $S$  given by  $S = R_1 / R_2$ , where  $R_1$  corresponds to the rate of the attack to GaAs and  $R_2$  the rate of attack to  $\text{Al}_x\text{Ga}_{1-x}\text{As}$ . The ideal solution should have a maximum in  $R_1$ , while  $R_2$  must be as low as possible.

## II. EXPERIMENTAL SET UP AND ETCHING SOLUTION

The preparation of the crystal begins by polishing it mechanically to a thickness around  $100 \mu\text{m}$ . For that, it must be fixed on a sapphire substrate (good hardness and optical quality), with a glue that supports the chemical attack and it should not block the light at the spectral region of interest. We have used the Zyvac 600 (non corrosive electronic epoxy). After the sample has been glued to the sapphire, it is necessary to cure the adhesive for approximately 1 hour at around  $100^\circ \text{C}$ . The corrosive solution that we used was composed by  $\text{H}_2\text{O}_2$  at 30 % and ammonia peroxide ( $\text{NH}_4\text{OH}$ , 58 %) <sup>3,4</sup>, the concentration of the solution being given by the volume fraction of the components  $\gamma = V(\text{H}_2\text{O}_2) / V(\text{NH}_4\text{OH})$ . Typically we have used for the etching a ratio of  $\gamma = 60$ . In the etching process, the solution is stored in a reservoir and a mechanical pump directs a fixed jet solution into the sample. Both typical area of the sample and the transversal section of the jet have  $0.5 \text{ cm}^2$  approximately. The sample area that can be processed by the etching system is limited by the aperture of the tubelike component placed between the sample (Fig. 1c) and the photo-

detector. Thus, the diameter of the tubelike component should be larger than the sample area. Moreover, the transversal area of the light beam should illuminate all sample area.

A jet of the etching solution ( $\text{H}_2\text{O}_2 + \text{NH}_4\text{OH}$ ) is obtained with an electromechanical pumping device (PQR-1/115, from Greylor Company), and produces a corrosive rate of  $\sim 2 \mu\text{m}/\text{min}$  in good agreement with Lepore's characterization results<sup>3</sup>. The etching solution is recovered in a closed circuit system, and it must be kept at low temperature in an ice bath to avoid the solution heating. The attack rate depends on both the concentration and temperature of the solution, and the dynamics of the jet solution in relation to the sample<sup>3</sup>. The experimental setup of the electromechanical jet system is illustrated in Fig. 1. The electronic control is shown on Fig. 1a and Fig. 1b. In Fig. 1c, we have all the etching system components: (1) etching solution, (2) reservoir box, (3) mechanical pump, (4) jet of the polishing solution, (5) sample, (6) lens, (7) powermeter, (8) electronic control system, and the laser light (780nm). The etching controlling system is made basically by a differential circuit, which compares the electrical signal (comparator-relay circuit - CRC) from the detector with a pre-adjusted reference set point in the range of the laser light power intensity from  $\mu\text{W}$  to  $\text{mW}$ . The circuit activates the relay when the detector signal (7) is larger than the reference one, which turn off the electromechanical pump (3). The set point is adjusted to be approximately the same signal from the detector, when there is no substrate to be etched. We have used a powermeter (Newport – model 835), which have a high sensitivity (pW to mW), which permitted to monitor the etching in a real time. All parts of the system were mounted in an acrylic box. The detector and jet tube were fixed with PVC material to avoid the attack of the etching solution.

The jet is injected close to a normal direction of the sample surface, together with a laser light beam (Fig. 1c). The jet solution and the laser beam are directed to the center of the sample, and a light detector is assembled behind the sample. The photodetector signal is analyzed by the powermeter, and it

is connected to an electronic controlling system (detail (8) in Fig. 1c), which stops the electromechanical pumping when the laser light reaches the detector passing through the etched sample. This controlling signal can be adjusted to suppress the jet to interrupt the etching process with a depth resolution of the order of nanometers (Fig. 1b), since the transmitted light across the sample becomes significant when the remaining layer of GaAs is closed to 100 nm thick. In our samples, after the GaAs substrate has a AlGaAs layer that works as a stop layer, since the selective of AlGaAs is bigger than GaAs (Fig. 3). Therefore, when the GaAs thickness decreases less than 100 nm, the laser light increases until a maximum intensity. Finally, the GaAs remaining cap layer of a few nanometers is etched with a jet solution of low concentration that guarantees us a reflected surface, which indicates a good quality of the etching process (Fig. 2). In the case of the semiconductors heterostructures that have partial selectivity, the etching system still can be useful. However, the electronic circuit must have a better adjustment to detect the light intensity transmitted through the desired thickness. The advantages of the etching system are the small contact of the operator with the chemical solution, the small quantity of used solution, greater independency of the system operator and a higher precision in the end point of attack mainly when semiconductor structure sample has low selectivity. Moreover, the jet solution pressure on the GaAs substrate permits both the better selectivity and a faster etching process in relation to the wet etching technique.

### III. SOME APPLICATIONS

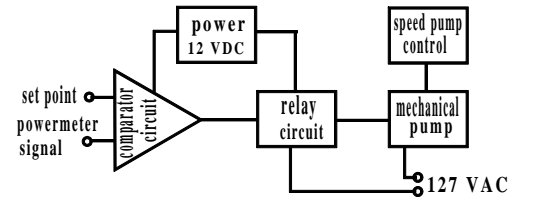
#### A. AlGaAs film

As the first example of the utility of the technique of selective etching we present the studies of optical absorption in films of  $\text{Al}_x\text{Ga}_{1-x}\text{As}$  in a system  $\text{Al}_x\text{Ga}_{1-x}\text{As}/\text{GaAs}$ . This system is largely used in opto-electronics and microelectronics, as an active medium and in building lattice matched heterostructures<sup>5</sup>.

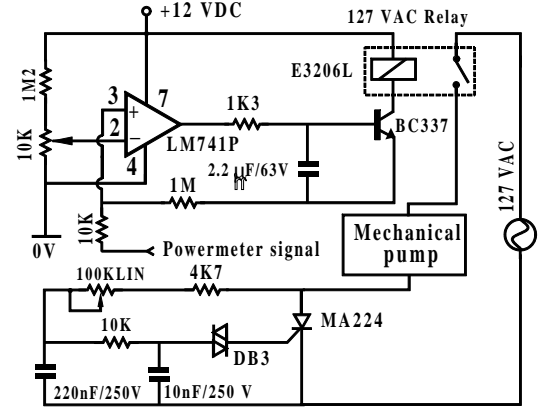
Recently, studying ultra-fast gap dynamics of  $\text{Al}_x\text{Ga}_{1-x}\text{As}$  near the crossover we have faced the difficulty of finding in the literature a variety of relations of energy gap  $E_{gap}(x)$  versus composition for the  $\text{Al}_x\text{Ga}_{1-x}\text{As}$  alloy<sup>6</sup>. In the indirect gap region the data are also scarce<sup>7</sup>. The problems arise in comparing literature data obtained by different  $E_{Gap}$  dependencies and we decided to measure the absorption of the samples that we were studying.

The films were grown by molecular beam epitaxy (MBE) over substrates of GaAs (001). A layer of AlAs of 500 Å (etching stop layer) was grown between the substrate and the  $\text{Al}_x\text{Ga}_{1-x}\text{As}$  layer. Above it was grown a 50 Å cap layer of GaAs to protect the sample against oxidation (see Fig. 3). We studied three  $\text{Al}_x\text{Ga}_{1-x}\text{As}$  samples with thickness of 150 nm ( $x=0.37$ ), 180 nm ( $x=0.43$ ), and 370 nm ( $x=0.45$ ).

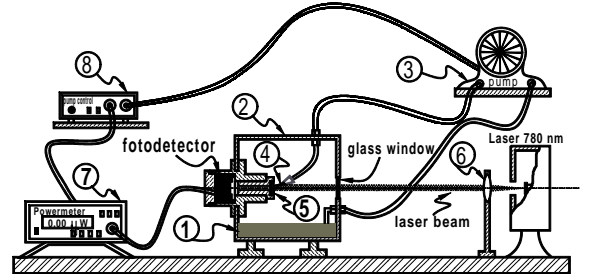
For the  $\text{Al}_x\text{Ga}_{1-x}\text{As}$  when the aluminium concentration increases the direct band gap changes from 1.42 eV (GaAs) to 2.78 eV (AlAs). Then, when the substrate of GaAs is almost



(a)



(b)



(c)

FIG. 1: (a) Bloch diagram for the etching system; (b) Electronic control circuit of the pumping system. The upper part of the circuit is the comparator-relay circuit and the lower part is the flow control circuit of the jet pumping; (c) Schematic of the electromechanical jet etching system.

removed, it is possible to see red light being transmit through the film. That is the reason why red light can be used to monitor the chemical etching.

By using the method described in the sections 2 and 3 we prepared the three samples for absorption studies. In Fig. 4, we present the absorption spectrum measured in the  $x=0.37$



FIG. 2: Details of a microcavity sample photo (1,5x1,1 mm) which shows the partial etching process (see Fig. 6). The black area is the GaAs substrate and the clear area is the AlAs surface without GaAs that was removed by the etching solution jet.

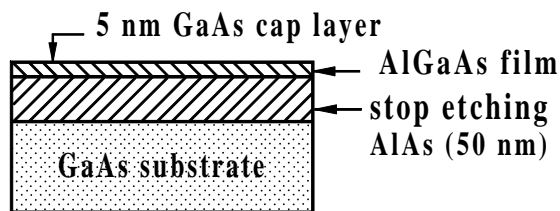


FIG. 3: Sample structure grown by MBE.

sample for different temperatures. At low temperatures we can even observe the presence of excitonic resonance that are due to Coulomb electron-hole interaction. As the temperature of the sample is lowered the exciton energy becomes greater than thermal energy and we can observe the exciton resonance. As the temperature increases the resonance broadens mainly due to phonon collisions.

We observe the excitonic resonance at low temperatures for all studied samples (Fig. 5). We note also that the excitonic peak of the  $x = 0.37$  sample (direct gap) is more pronounced than the indirect ones and that the absorption edge shifts to higher energies as the aluminium concentration of the samples increases.

From the measurements at 15 K we can determine the direct gap. This is accomplished summing the exciton binding energy ( $7 \text{ meV}$ )<sup>8</sup> to the peaks observed experimentally to determine the gap, i.e.,  $E_g = E_{lig.exc} + E_{pico}$ . The following table 1 presents the gaps of the studied sample obtained from the last energy relation. Once again, these results illustrate both the importance and the resolution of this developed etching system, since we have studied at most one thin film Al-

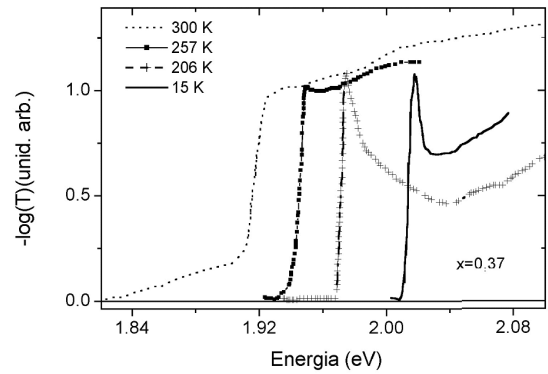


FIG. 4: Absorption spectrum of the  $\text{Al}_x\text{Ga}_{1-x}\text{As}$  sample ( $x=0.37$ ) as a function of the temperature.

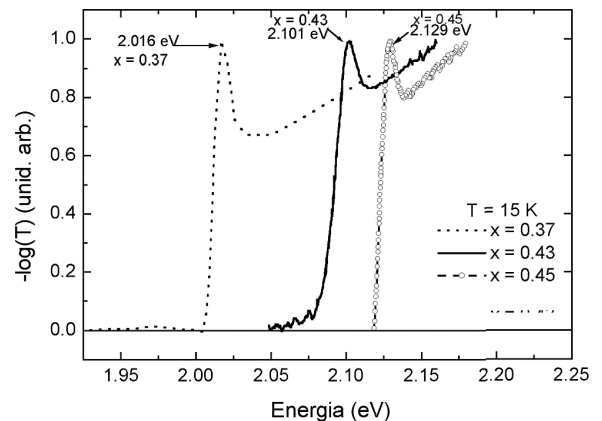


FIG. 5: Absorption spectrum at 15 K of the three  $\text{Al}_x\text{Ga}_{1-x}\text{As}$  samples with different aluminium concentrations.

GaAs/AlAs of 400 nm of thickness. If there is 100 nm of GaAs substrate at least, our transmitted signal would be absorbed in the substrate, and it would not be possible to have these optical datas<sup>1</sup>

Table 1 - Direct gap determination from the absorption measurements at 15 K

$x$	$E_g(\text{eV})$
0.37	2.023
0.43	2.108
0.45	2.136

### B. Microcavity

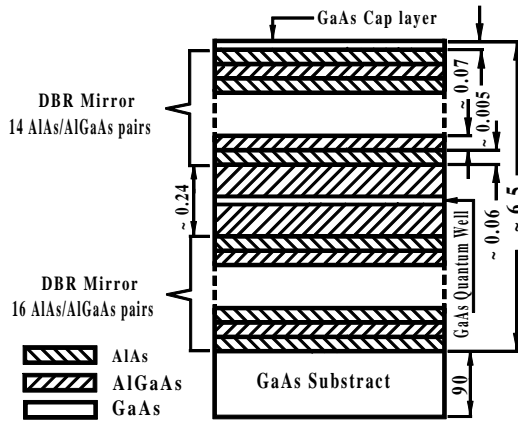


FIG. 6: A  $\lambda$  GaAs microcavity sample structure grown by MBE. The linear measurements are in micrometers.

This etching process is applied in many laser system as delicate as one GaAs microcavity, in order to remove the GaAs substrate. A typical GaAs microcavity structure is shown in Fig. 6. The cavity is formed by two distributed Bragg refractor mirror (DBR) with one quantum well in the center, in order to match the position of the gain media and the electro magnetic field antinode position.<sup>9</sup>

The DBR mirror reflectivity is extremely sensitive to the AlGaAs/AlAs pair number and layer configurations. The mirror reflectivity can be estimated from the Fabry-Pérot resonance width at half maximum (FWHM)  $\delta^{10}$  given by

$$\delta = \frac{c \left( \alpha - \frac{1}{l} \ln \sqrt{R_1 R_2} \right)}{2\pi n},$$

where  $c$  is the light velocity,  $l$  is the cavity effective length,  $n$  is the refraction index,  $\alpha$  is the cavity loss, and  $R_{1,2}$  is the cavity mirror reflectivity. In Fig. 7a, we show the reflectance spectrum of the microcavity at room temperature obtained with white light and normalized with the white light source reflectance spectrum of a aluminum mirror in order to correct the spectrometer gain curve as well as the white light source intensity variation with wavelength. We measured  $\delta_i = 5$  nm and estimated  $R = 0.96$  for this microcavity. After the sample etching, we measured the transmitted spectrum with the white light source. From Fig. 7b, we measured the cavity resonance FWHM  $\delta_f = 9$  nm. We estimated again the cavity mirror reflectance and obtained  $R = 0.93$ , showing us a broader cavity

window and lower reflectivity if compared with the initial value. It means that the etching process have stopped very close to the first DBR layer, but not enough, since the lower reflectance shows us an introduction of loss in one of the cavity DBR mirror, which results in a lower cavity finesse.

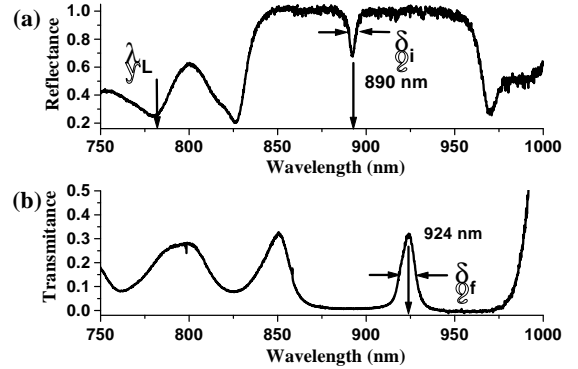


FIG. 7: (a) Reflectance spectrum obtained with white light source from the GaAs substrate microcavity with resonance window at 890 nm. The laser light at  $\lambda_L=780$  nm was used as a probe for the etching system process; (b) Transmission curve for the same microcavity sample, after removed the substrate, showing the resonance at 924 nm.

### IV. CONCLUSION

We have constructed a jet etching system for etching Al-GaAs/GaAs semiconductor heterostructures with a resolution of few nanometers thickness. The resolution is demonstrated in the attack of the thin film of AlGaAs (in order of 100 nm), since the area of the sample is much bigger than its thickness. Moreover, we can follow the color change of the sample that guarantees us a resolution of a few nanometers. This etching system is presented here with some applications and results for absorption experiments. The etching power is illustrated with some primary applications in absorption spectroscopy of AlGaAs films, and also of GaAs microcavity.

### V. ACKNOWLEDGEMENT

We acknowledge R. R. Menezes for his technical support and financial support given by CNPq, PRONEX, SEBRAE and Milênio Institute of Nanoscience

[1] L. H. F. Andrade, R. Marotti, Alain A. Quivy, C. H. Brito Cruz, “Interplay between direct gap renormalization and intervalley scattering in AlxGa1-xAs near the Gamma-X crossover”, Solid State Commun. **121**, 181-185 (2002).

[2] M. A. Sagiore, “Interferência quântica em cavidades de baixa finesse”, tese de doutorado, UFMG, Belo Horizonte (2004).

[3] J. J. Lepore, “An improved technique for selective etching of GaAs and Ga1-xAlxAs”, J. Appl. Phys. **51**, 6441-6442 (1980).

- [4] R. A. Logan, F. K. Reinhart, "Optical waveguide in GaAs/AlGaAs epitaxial layers", J. Appl. Phys. **44**, 4172-4176 (1973).
- [5] Jasprit Singh, *Semiconductor Optoelectronics-Physics and Technology*, MacGraw-Hill, pp. 443 (1995).
- [6] L. Pavesi, M. Guzzi, "Photoluminescence of Al<sub>x</sub>Ga<sub>1-x</sub>As alloys", J. Appl. Phys. **75**, 4779-4842 (1994).
- [7] S. Lassen, R. Schwabe, J. L. Staehli, "Indirect-gap Al<sub>x</sub>Ga<sub>1-x</sub>As and its similarity to gap", Semicond. Sci. Technol. **10**, 903-913 (1995).
- [8] H. Kalt, M. Rinker, "Band-gap renormalization in semiconductors with multiple inequivalent valleys", Phys. Rev. B **45**, 1139-1154 (1992).
- [9] Y. Yamamoto, S. Inoue, H. Heitmann, G. Bjork, and F. M. Matinaga, "Quantum Optics Effects in Semiconductor Lasers", book chapter of: *Semiconductor Lasers I: Fundamentals*, pp. 361-441, Edited by Eli Kapon, Academic Press, San Diego CA-USA, 1999.
- [10] A. Yariv, *Quantum Electronics*, Chap.7, Ed. By John Wiley & Sons, New York, USA 1987.